CrystEngComm

Accepted Manuscript

ROYAL SOCIETY OF CHEMISTRY

www.rsc.org/crystengcomm

Journal Name

RSCPublishing

ARTICLE

Coordination Environments and π-Conjugation in Dense Lithium Coordination Polymers†

Cite this: DOI: 10.1039/x0xx00000x

Satoshi Tominaka,[*a,b] Hamish H.-M. Yeung,[a] Sebastian Henke[c] and Anthony K. Cheetham[*b]

Received 00th January 2012,
Accepted 00th January 2012

DOI: 10.1039/x0xx00000x

www.rsc.org/

Understanding of lithium oxygen coordination systems is important for making better lithium conductors as well as active materials for lithium ion batteries. Here we report a systematic investigation on coordination environments in lithium coordination polymers (LCPs) through the syntheses and analyses of six new crystals composed of lithium ions and anthraquinone (aq) derivative anions, where the negative charges are distributed in π-conjugation systems. Their structures were determined by single-crystal X-ray diffraction as (**1**) [Li_2(23dcaq)(H_2O)] in space group $P2_1/c$, (**2**) [Li(23dcaqH)] in $P2_1/c$, (**3**) [Li_2(15dhaq)(H_2O)$_2$] in $P2_1/c$, (**4**) [Li_2(14dhaq)(H_2O)$_2$] in *Pnma*, (**5**) [Li(14dhaqH)(H_2O)] in $P2_12_12_1$, and (**6**) [Li(14hnaq)(H_2O)] in $P2_12_12_1$ (23dcaq^{2-} = 2,3-dicarboxy-aq, 14dhaq^{2-} = 1,4-dihydroxy-aq, 15dhaq^{2-} = 1,5-dihydroxy-aq and 14hnaq^{-} = 1-hydroxy-4-nitro-aq). Through the comprehensive structure analysis of these materials as well as other LCPs, we found that when considering the longest C-O bond in the π-conjugation system of an anionic organic molecule and its coordination to a Li ion, there is a weak inverse relationship between the C-O and Li-O bond length. In addition, despite exhibiting optical band edges below 2 eV and 1-D π-stacking connectivity, conductivity measurements on single crystals of **1**-**6** confirmed that they are all electronic insulators. We rationalize this finding on the basis of π-orbital delocalization, which is more restricted in the aq-based LCPs compared to known semiconducting hybrid materials.

1. Introduction

Inorganic materials such as oxides and carbons are widely used as electrode materials for lithium ion batteries,[1] while organic and hybrid materials are also promising for future batteries.[2, 3] For example, lithium tetrahydroxybenzoquinone hybrids ($Li_xC_6O_6$)[2, 4, 5] and lithium conjugated-dicarboxylate materials such as dilithium terephthalate ($Li_2C_8H_4O_4$) have been investigated as electrode materials.[6, 7] These lithium coordination polymers (LCPs) utilize π-conjugated organic molecules instead of transition metal coordination polyhedra (e.g., CoO_6 octahedra) and thus are attractive in terms of "materials sustainability",[6] namely, materials production using abundant organic resources through environmentally friendly processes. For the successful application of LCPs in batteries, better understanding of Li-O coordination environments and charge distributions through π-conjugation systems are necessary. For example, for rapid Li^+ conduction, weak coordination (e.g., long Li-O bonds) as well as the presence of vacant sites is favourable.[8]

There are several families of LCPs and most of them are dense structures with simple mono-carboxylate linkers, such as formate[9] and acetate,[10, 11] or dicarboxylate linkers such as oxalate,[12] tartrate[13-15] and terephthalate.[16] Microporous LCPs, or lithium-organic frameworks, are also being actively developed as a lightweight group of metal-organic frameworks (MOFs) for gas sorption application.[17-19] Li-O bonds are ionic in nature in oxides, and this is considered to be true also in LCPs.[20] If there are π-conjugation systems in LCPs, the negative charges on the oxygen atoms may be delocalized, and thus the nature of the chemical bonds (e.g., single bonds/double bonds) in the organic molecules are determined by the charge distribution. Charge redistribution through π-conjugation and associated bond reformation are typical for carboxylate groups, where the C-O bond lengths depend on the distribution of the one negative charge in the group.[21] This is analogous to that in transition metal coordination polyhedra in classical oxides.[22]

In order to acquire a better understanding of Li-O coordination environments in LCPs and their influence on the π-conjugation in the organic molecules, we herein investigate LCPs consisting of rigid and bulky linkers of anthraquinone (aq) derivatives (Scheme 1), whose π-conjugated systems are sensitive to the electronic environment of the keto groups on the centre ring. Thus, coordination of the keto groups with lithium is expected to strongly affect the bond lengths of the aq derivatives, and the charge distribution in the aq may also

influence the Li-O coordination spheres. Other conjugated substituents, such as hydroxyl, carboxylate and nitro groups, are also expected to influence the electronic environment to varying degrees. We have therefore synthesized a series of LCPs based on anthraquinone derivatives, determined their structures by single-crystal X-ray diffraction, and measured their photoabsorption spectra and conductivities. The results provide a better understanding of Li-O coordination environments and their influence on π-conjugated systems in LCPs.

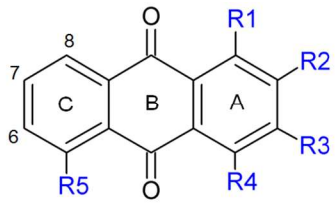

14dhaqH$_2$ (R1, R4 = OH)
15dhaqH$_2$ (R1, R5 = OH)
23dcaqH$_2$ (R2, R3 = CO$_2$H)
14hnaqH (R1=OH, R4 = NO$_2$)

Scheme 1 Substitution patterns of anthraquinone derivatives composed of three six-membered rings studied in this work: 2,3-dicarboxyanthraquinone (23cdaqH$_2$), 1,4-dihydroxyanthraquinone (14dhaqH$_2$), 1,5-dihydroxyanthraquinone (15dhaqH$_2$), and 1-hydroxy-4-nitro-anthraquinone (14hnaqH).

2. Experimental

2.1 Synthesis

Crystals of anthraquinone derivatives with lithium ions were synthesized under solvothermal conditions from lithium hydroxide (LiOH·2H$_2$O from Fisher) or lithium acetate (LiOAc·2H$_2$O from Fisher) and anthraquinone derivatives (all from TCI): (*i*) 1,4-dihydroxyanthraquinone, "14dhaqH$_2$"; (*ii*) 1,5-dihydroxyanthraquinone, "15dhaqH$_2$"; (*iii*) 2,3-dicarboxyanthraquinone, "23dcaqH$_2$"; and (*iv*) 1-hydroxy-4-nitroanthraquinone, "14hnaqH". As solvents, ethanol (>99.8% from Fisher), deionized water (reagent grade from Fisher) and acetonitrile (HPLC grade from Fisher) were used.

[Li$_2$(23dcaq)(H$_2$O)], 1: 23dcaqH$_2$ (1 mol L^{-1}) and LiOH (2 mol L^{-1}) were dissolved in water (8 mL), treated by ultrasonication for 20 sec, heated at 60°C for 1 h, and then kept at 90°C overnight in a loosely sealed glass vial in order to dry up gradually. The chemical composition was determined by elemental analysis at Department of Chemistry, University of Cambridge: (found, calc'd in wt%), C (58.81, 58.93), H (2.45, 2.45), N (0.00, 0.00). The H$_2$O content was determined by thermal analysis (see Fig. S1): (found, calc'd in wt%), (6.3, 5.5). **1** crystallizes in pale yellow plates. The colour is the same as that of pure organic linker molecules by eye.

[Li(23dcaqH)], 2: 23dcaqH$_2$ (10 mmol L^{-1}) and LiOAc (20 mmol L^{-1}) were dissolved in acetonitrile (20 mL), treated by ultrasonication for 20 sec, and then heated at 100°C for 2 days in a loosely sealed glass vial. During the heating process, acetonitrile was gradually dried up. The product was rinsed with ethanol and then dried. For the structure determination, the solution was heated in a well-sealed borosilicate glass vial overnight, and bigger crystals were grown. The pale yellow block crystals were recovered filtration under reduced pressure, rinsed with ethanol, and then dried in air. Elemental analysis: (found, calc'd), C(60.21, 64.02), H (2.43, 2.33), N(0.00, 0.00). This error in the elemental analysis suggests the presence of other phases because the precursor stoichiometry does not match the product, or because of hydrolysis. H$_2$O content: (found, calc'd in wt%), (0.7, 0.0). **2** crystallizes in pale yellow blocks. The colour is the same as that of pure organic linker molecules by eye.

[Li$_2$(15dhaq)(H$_2$O)$_2$], 3: 15dhaqH$_2$ ethanol solution (75 mmol L^{-1}) and LiOH aqueous solution (1.53 mol L^{-1}) were mixed in 1 :1 volume ratio (8 mL). The solution was heated at 90°C for 3 days in a well-sealed borosilicate glass vial, and then kept at room temperature for a few days. Crystals were recovered by vacuum filtration, rinsed with ethanol, and then dried in air. Elemental analysis: (found, calc'd), C(56.49, 58.36), H(3.39, 3.47), N(0.00, 0.00). H$_2$O content: (found, calc'd in wt%), (12.0, 12.5).

[Li$_2$(14dhaq)(H$_2$O)$_2$], 4: 14dhaqH$_2$ ethanol solution (23 mmol L^{-1}) and LiOH aqueous solution (60 mmol L^{-1}) were mixed in 1 : 1 volume ratio (8 mL). The solution was heated at 90°C for 2 days in a well-sealed borosilicate glass vial, and then kept at room temperature for a few days. Crystals were recovered by filtration under reduced pressure, rinsed with ethanol, and then dried in air. Elemental analysis: (found, calc'd), C(59.03, 58.36), H(3.41, 3.47), N(0.00, 0.00). H$_2$O content: (found, calc'd in wt%), (12.5, 12.8).

[Li(14dhaqH)(H$_2$O)], 5: 14dhaqH$_2$ (200 mmol L^{-1}) and LiOH (210 mmol L^{-1}) were dissolved in water (8 mL). The solution was heated at 90°C for 2 days in a well-sealed borosilicate glass vial, and then kept at room temperature for a few days. The blackish-red needles were recovered by vacuum filtration, rinsed with ethanol, and then dried in air. Elemental analysis: (found, calc'd), C(63.19, 63.65), H (3.33, 3.41), N(0.00, 0.00). H$_2$O content: (found, calc'd in wt%), (7.6, 6.8).

[Li(14hnaq)(H$_2$O)], 6: 14hnaqH (12 mmol L^{-1}) and LiOH (60 mmol L^{-1}) were dissolved in water (8 mL). The solution was heated at 90°C for 3 days in a well-sealed borosilicate glass vial, and then was gradually cooled down to room temperature. The crystals, clear deep red needles, were recovered by vacuum filtration, rinsed with ethanol, and then dried in air. Elemental analysis: (found, calc'd), C(57.80, 57.36), H(2.73, 2.73), N(4.76, 4.78). The H$_2$O content was determined by thermal analysis (cf. Fig. S1): found 6.2 wt%; calc'd, 6.1 wt%. Note that the occupancy of the H$_2$O site in the structure determined by single crystal X-ray diffractometry at room temperature was found to be 0.21. This is probably due to partial dehydration during the X-ray diffraction measurements, considering that this compound dehydrates even at room temperature (Fig. S3).

[Li(HCO$_2$)]: Large crystals of anhydrous lithium formate were synthesized by a solvothermal reaction. LiOH (4 mol L^{-1}) was treated by sonication in 8 mL of N,N-dimethylformamide (DMF) for 20 min. After adding imidazole (3.9 mol L^{-1}), the solution was further treated by sonication for 1 h, then kept at 90°C for 2 days. Rod-like crystals (0.1–1 mm) were obtained. Elemental analysis: (found, calc'd), C(22.04, 23.12), H(2.12, 1.92), N(0.63, 0.00). The nitrogen contamination is possibly from dimethyl ammonium cations generated by the decomposition of DMF.

2.2 Structure determinations

The crystal structures of compounds **1-6**, Li(HCO$_2$) and the free ligand 14hnaqH were determined by single crystal X-ray diffractometry at 120 K and room temperature (details are available in the ESI). The structures were solved by direct methods and were then refined by the method of least squares

minimization using the SHELX program[23] within the Olex2 interface.[24] All non-hydrogen atoms were refined anisotropically and hydrogen atoms were refined isotropically. Hydrogen atoms on anthraquinone-derived molecules and the hydroxyl groups were added at geometrically reasonable positions and refined using riding models (AFIX43 and 147). Those on carboxylic acid were added at chemically reasonable positions found in the Fourier difference maps and then refined without constraints. Those on water molecules were added likewise, and then refined with constrained O-H distances (0.958Å) and H-O-H angles (104.5°) taken from the water molecule.[25] Visualization of structures and calculation of effective coordination numbers were carried out using the VESTA program[26] and π-stacking was analysed using the Mercury program.[27] CIF files are available for the structures described herein.‡ Other analyses, including thermogravimetric analysis (Fig. S1-S4), powder X-ray diffraction (Fig. S5 and Table S1), and infrared spectroscopy (Fig. S6 and S7), were carried out to support the single crystal analysis, as shown in the ESI.

3. Results and discussion

3.1 Relationship between Li-O bond length and C-O bond length and other structural features in LCPs

We analyzed various structural features of LCPs, including lithium tartrates,[13-15] lithium malates,[28] lithium dimethyl succinate,[29] lithium formate anhydrate and monohydrate,[9] dilithium terephthalate,[16] lithium oxalate,[12] dilithium malonate,[30] dilithium squarate,[7] lithium acetate dihydrate,[10] dilithium carbonate,[31] as well as the new structures containing anthraquinone derivatives. The structural features included bond lengths, framework dimensionality, polyhedral connectivity, Li coordination environment, Li-O tetrahedral distortion (δ_{tet}) and effective coordination number (ECoN), and π-π stacking. These features were chosen due to their potential relevance to ionic and/or electronic conductivity, as discussed subsequently. A summary can be found in Tables S2-6 and Figure S8 in the ESI.

We examined the correlation between the longest C-O bond lengths in the π-conjugated systems of interest and the shortest Li-O coordination bonds, as shown in Fig. 1. The correlation is quite weak (dotted line and red plots in Fig. 1), but as the C-O bonds become longer, the Li-O bonds become shorter. C-O lengths are known to reflect π-conjugation states (~1.20 Å for sp^2-sp^2 double bonds, ~1.27 Å for conjugated sp^2-sp^2 bonds in carboxylate ions, and ~1.35 Å for single bonds),[32] and thus shorter C-O bonds indicate less negative charge in the π-conjugated systems (*i.e.*, more neutral bonds) and longer C-O bonds mean more negative charge on the O atoms. That is, the more negatively charged oxygen atoms tend to be closer to the Li^+ ions. This is reasonable considering the local charge neutralization and the long Li-O bond lengths for coordinated water molecules (*i.e.*, longer than the Li-O-C bonds, in general).

Exceptions are found when the Li-O bonds are not the shortest ones in the coordination spheres, when the effective coordination numbers (ECoNs; defined as summation of the bond weight)[33] of Li ions are above 4.0, and when the C-O groups have hydrogen bonding. The 1st exception is often found in structures having high inorganic dimensionalities, such as I^3O^0 of lithium formate anhydrate and lithium carbonate, and I^2O^1 of lithium dimethyl succinate and dilithium oxalate, probably suggesting that these coordination spheres are not dominated by one anionic group, but rather formed by shielding the localized positive charge of Li^+ ions with delocalized charges of multiple anions. The 2nd exception is simply due to the influence of steric hindrance on the Li-O coordination spheres, and the 3rd is a result of protons dominating the local charge distribution. Therefore, the weak correlation we found is applicable when the LiO_4 coordination is dominated by the negative charge of one coordinating group.

Regarding the Li coordination spheres, when other features such as ECoN, tetrahedral distortion and connectivity were examined (Table S2-S4), no other general correlations between Li-O coordination and size/flexibility of organic linkers were apparent. This may be a result of the diversity in composition (degree of lithiation and hydration, linker geometry, flexibility and stereochemistry etc.), which strongly affects non-systematic variations in the Li-O bonding.

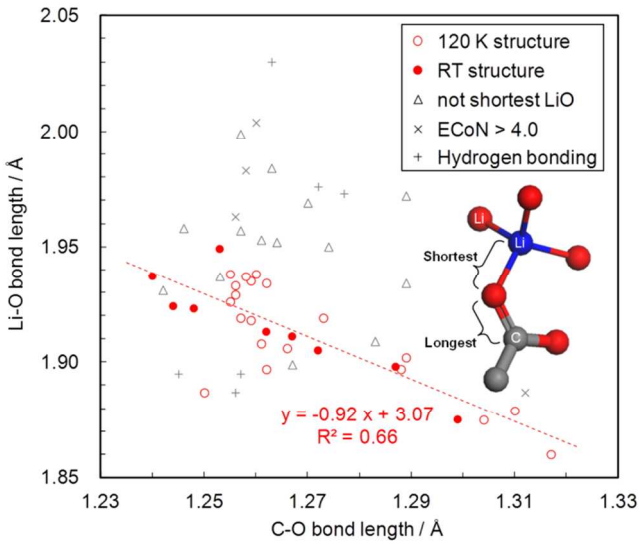

Fig. 1 Relationship between the longest C-O bond length in the π-conjugated system of an organic acid anion in a LCP and its coordination bond length to Li ions. When the Li-O bonds are the shortest ones in the coordination spheres, there is a weak correlation, shown as a dotted line (linear approximation for the open and closed circle plots). The inset illustrates an example of a carboxylate system. Open circles: data obtained from structures determined at 120 K (tartrates, malates, dimethyl succinate, and formate as well as the anthraquinone derivatives). Closed circles: data obtained from structures determined at room temperature (terephthalate, formate, oxalate, malonate, squarate, acetate, and carbonate as well as the anthraquinone derivatives). Triangles: the C-O bonds not having the shortest Li-O bonds. The structures are those mentioned above (120 K and RT). ×-marks: the data for the Li-O coordination spheres having effective coordination numbers (ECoNs) above 4.0. +-marks: the data for the C-O bonds having hydrogen bonding to the oxygen atoms.

In the following sections, we present structural analyses of the lithium anthraquinone derivatives, which have π-conjugated systems of different sizes. In addition to the C-O π-conjugation, anthraquinone derivatives have C-C π-conjugation, whose states can be investigated by measuring C-C bond lengths (in general, ~1.34 Å for non-aromatic sp^2-sp^2 carbon, ~1.39 Å for aromatic sp^2-sp^2 carbon, ~1.54 Å for sp^3-sp^3 carbon).[32] Thus, through the bond length analysis, we discuss the π-conjugation states of molecules in order to examine the charge distribution within them. This sheds further light on the correlation between the bond lengths in the organic molecules and the Li-O polyhedra.

3.2 Carboxyanthraquinone frameworks

Two new crystal structures containing 23dcaq and lithium were determined. One is a dilithium, monohydrated material, [Li_2(23dcaq)(H_2O)], compound **1** (Fig. 2), and the other is a monolithium, anhydrous phase, [Li(23dcaqH)], **2** (Fig. 3). **1** contains Li1-Li2-Li2-Li1 tetramers (Fig. 2a) connected by the linker molecules to form 2D structures (I^0O^2 following Cheetham *et al.*[34]) within the *bc* planes (Fig. 2b and 2c), with the A rings (Scheme 1) having carboxylate groups stacked along the *c*-axis.[35, 36] Such carboxylate groups are commonly considered to withdraw electrons from the aromatic rings, but the lengths of the C-C bonds and C-O keto bonds in **1** and **2** are the same as those in pure 23dcaqH_2 molecules (Fig. 2f), indicating that no charge redistribution in the anthraquinone rings happens upon LCP formation. The tilt angles of the carboxylate groups from the aromatic rings (by ~20° in **1,** top left, Fig. 2d; ~90° in **1**, bottom left, Fig. 2d; ~30° in **2**, top left, Fig. 3d; ~20° in **2**, bottom left, Fig. 3d) also indicate weak π-conjugation between them. Thus, we can consider the π-system of the carboxylate groups as essentially separate from the π-conjugation of the aq rings. This is considered to be generally true for 23dcaq-based coordination polymers, as shown in Fig. S10.[37]

Li1 ions in **1** (blue, Fig. 2) are coordinated by four oxygen atoms from two carboxylate groups, a keto group and a water molecule. The shortest Li-O bond (1.92 Å) is formed with the long C-O group (1.26 Å) of the bottom carboxylate in Fig. 2d. This follows the relationship in Fig. 1 (cf. Fig. S9). However, Li2 ions (purple, Fig. 2) are coordinated by five oxygen atoms (ECoN = 4.38) from four carboxylate groups and a H_2O molecule, and thus are an exception to the relationship. The other carboxylate group in Fig. 2d has a longer C-O bond (1.26 Å) and forms a Li-O bond of 1.96 Å, which is the shortest one for Li2. This is an outlier to the relationship shown in Fig. 1 and Fig. S9, due to steric hindrance caused by other oxygen atoms. In addition, these two coordination spheres confirm that the neutral ligand (*i.e.* H_2O) has longer bonds than the anionic ones (*i.e.*, -COO^-), and the polarisable but neutral π-conjugated groups (*i.e.*, -C=O) are in-between them.

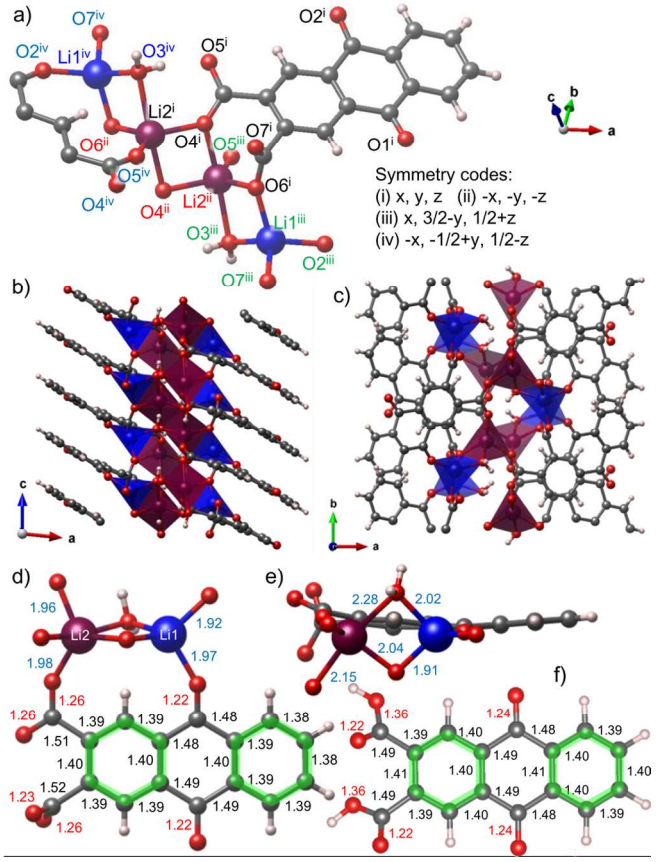

Fig. 2 Crystal structure of **1** [Li_2(23dcaq)(H_2O)]. H (white), Li (blue, purple), C (grey), O (red). (a) Li polyhedron tetramer connected by edge sharing. (b, c) The inorganic moiety extends across the *bc* plane. The anthraquinone units stack along the *c* axis. The inorganic layers are sandwiched by organic domains and stack along the *a* axis. Blue polyhedra = Li1, and red polyhedra = Li2. (d, e) Coordination environments and bond lengths determined at room temperature, compared with the 23dcaqH_2 structure determined by DFT calculations (f). The blue numbers are Li-O bond lengths in Å, the red ones are C-O bond lengths, and the black ones are C-C bond lengths. The green highlights illustrate strong π-conjugation in the C-C bonds close to the typical aromatic C-C bond length of 1.39 Å.

Compound **2** contains isolated, tetrahedral lithium ions connected by linker molecules to form 2D layers within the *bc* planes (Fig. 3a). The anthraquinone molecules are stacked along the *a* axis. Li ions are coordinated by four oxygen atoms from three carboxylate groups and a keto group. The longer C-O in the top carboxylate (1.27 Å) in Fig. 3d forms Li-O bond of 1.98 Å, and the longer C-O in the bottom one (1.28 Å) forms Li-O bond of 1.97 Å, but the shortest Li-O (1.91 Å) is formed with another carboxylate of 1.22 Å. Since this compound has hydrogen bonding between two carboxylate groups, the long C-O bonds do not reflect the negative charges shielding the positive charge of Li^+ ions, but rather reflect the hydrogen bonding. Thus, this is a typical example of an exception to the correlation when hydrogen bonding exists (Fig. S9).

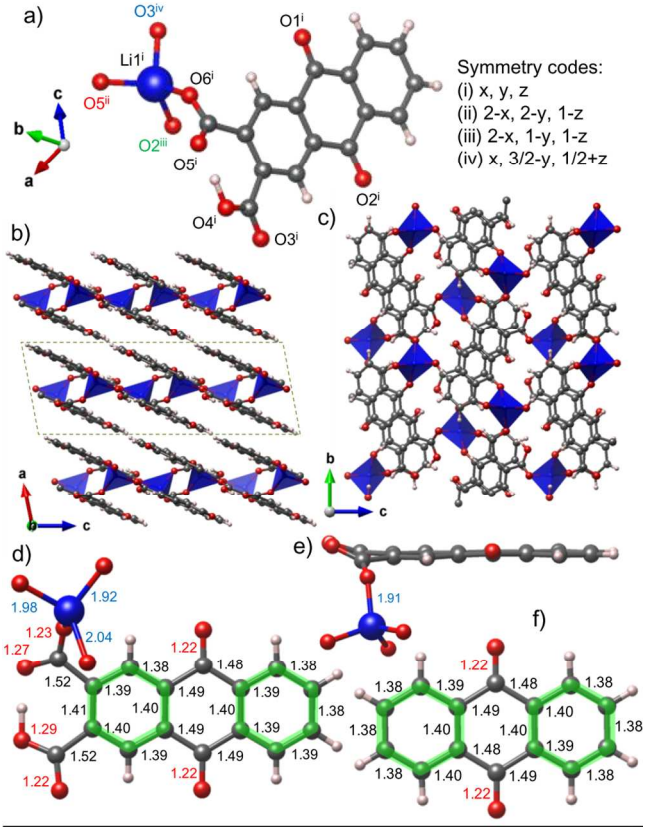

Fig. 3 Crystal structure of **2** [Li(23dcaqH)]. H (white), Li (blue), C (grey), O (red). (a) Li ions are coordinated by carboxylate and keto groups. One of the carboxylate groups is protonated. (b, c) The network extends across the *bc* plane and the anthraquinone parts stack along the *a* axis, as shown by the dashed box. (d, e) Coordination environments and bond lengths determined at room temperature, compared with the data of anthraquinone (f) from the Cambridge database (CSD ANTQUO08). The blue numbers are Li-O bond lengths in Å, the red ones are C-O bond lengths, and the black ones are C-C bond lengths. The green highlights illustrate strong π-conjugation in C-C bonds close to the typical aromatic C-C bond of 1.39 Å.

3.3 Hydroxyanthraquinone frameworks

Compared with the carboxy-anthraquinones, the hydroxyl groups form π-conjugation with the anthraquinone parts upon deprotonation, and thus the negative charges are considered to be delocalized across the π-conjugated systems. For example, 15dhaqH_2 is a dark yellow powder and becomes red when deprotonated (15dhaq^{2-}), and 14dhaqH_2 is an orange powder and turns purple when deprotonated (14dhaq^{2-}). Then, the colour further changes when they form LCP crystals: compound **3**, [Li_2(15dhaq)(H_2O)$_2$], appears dark green in reflection (Fig. 4a) and dark red in transmission, while **4**, [Li(14dhaqH)(H_2O)], appears dark orange in reflection (Fig. 5a) and dark red in transmission. Though the colours suggest narrow optical band gaps (1.6–3.2 eV, confirmed by optical absorption measurements; see Section 3.4 and Fig. S11), these compounds were found to be insulators by single crystal conductivity measurements.[38, 39]

Compounds **3** and **4** have similar connectivity and I^0O^1 dimensionality: anthraquinone molecules are connected by pairs of lithium ions (Fig. 4b and 5b), and these form 1D structures ~~(Fig. 4c and 5c)~~. This is reasonable in view of the planar structures of the organic linkers, and, interestingly, the anthraquinone units of a single chain are in the same plane to form ribbon-like structures, stacked along the *b* axis for **3** (Fig. 4c) and the *a* axis for **4** (Fig. 5c). Compounds **5**, [Li(14dhaqH)(H_2O)] (Fig. 6), and **6**, [Li(14hnaq)(H_2O))] (Fig. 7), have the same connectivity and I^1O^0 dimensionality, where anthraquinone molecules are connected by Li ion chains along the *a* axis. The anthraquinone molecules are stacked along the same direction, the *a* axis.

In these four structures, Li ions are coordinated by a phenoxide group, two keto groups, and a water molecule, except for **5**. The C-O bond lengths of the phenoxide groups are shorter (~1.30 Å) than in the protonated pure linkers (~1.35 Å), and those of the keto groups are slightly longer (~1.25 Å) than the linkers (~1.23 Å), except in **6**. Taking the C-C bond lengths into consideration, the negative charges of **3**–**5** are delocalized mainly in the phenoxide rings and the oxygen atoms, but slightly in the C-C and C-O bonds in the centre rings, while those of **6** are solely in the phenoxide rings and the oxygen atoms. In these conjugation systems, the longest C-O bonds are the phenoxide ones, and they form the shortest Li-O bonds in **3** and **4**, and these are shown at the right bottom in Fig. 1 (cf. Fig. S9) and follow the relationship. In addition, the molecular complex of [Li_2(dhaq)(H_2O)$_5$] (**7**), having I^0O^0 dimensionality, also follows the relationship (Fig. S12 in ESI). The ECoN of the Li coordination in **5** is 4.2, and the plot in Fig. 1 and S9 is slightly off the correlation, as shown as the ×-mark at the right bottom. In **6**, the shortest Li-O bond is formed with the keto group, and this is the left bottom +-mark, which is far from the linear correlation.

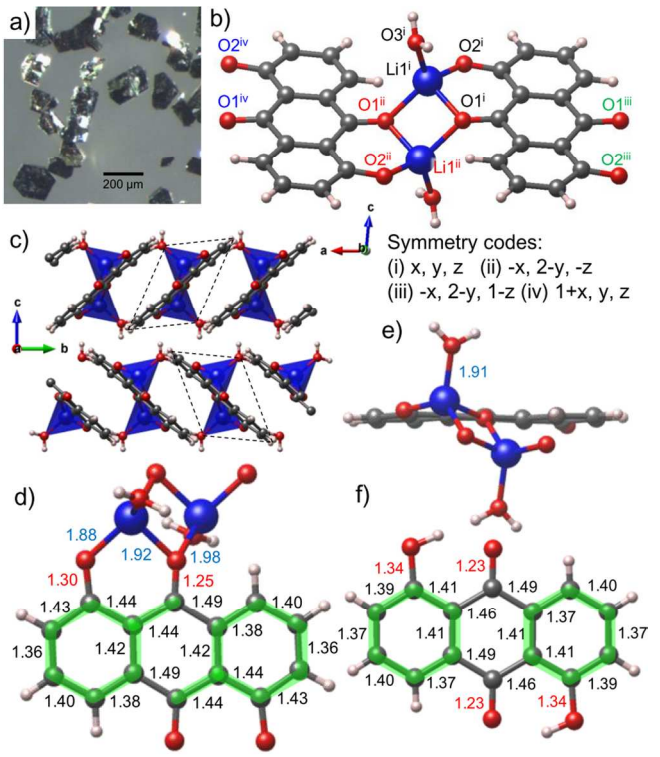

Fig. 4 Micrograph and crystal structure of **3** $[Li_2(15dhaq)(H_2O)_2]$. (a) Optical microscope image. (b) LiO_4 dimers are formed between two 15dhaq linkers. H (white), Li (blue), C (grey), O (red). The dimers and linker molecules form 1D chains. The anthraquinone parts of one chain are connected along the *a* axis (ribbon-like structures). (c) The chains are arranged in parallel along the *b* axis as shown by the dashed boxes (d, e) Coordination environments and bond lengths determined at room temperature, compared with the data for a protonated linker molecule (f) from the Cambridge database (CSD DHANTQ02). The blue numbers are Li-O bond lengths in Å, the red ones are C-O bond lengths, and the black ones are C-C bond lengths. The green highlights illustrate strong π-conjugation in C-C bonds close to the typical aromatic C-C bond of 1.39 Å.

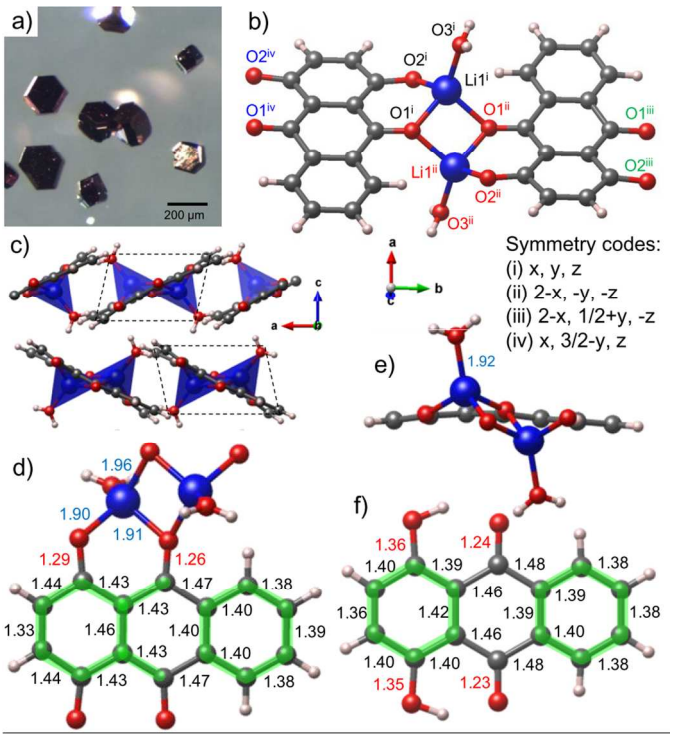

Fig. 5 Micrograph and crystal structure of **4** $[Li_2(14dhaq)(H_2O)_2]$, isostructural connectivity with **3**. (a) Optical microscope image. (b) LiO_4 dimers are formed between two 14dhaq linkers. H (white), Li (blue), C (grey), O (red). The dimers and linker molecules form 1D chains. The anthraquinone parts of one chain are connected along the *b* axis (ribbon-like structures). (c) The chains are arranged in parallel along the *a* axis as shown by the dashed boxes. (d, e) Coordination environments and bond lengths determined at room temperature, compared with the data of a protonated linker molecule (f) from the Cambridge database (CCDC 106210). The blue numbers are Li-O bond lengths in Å, the red ones are C-O bond lengths, and the black ones are C-C bond lengths. The green highlights illustrate strong π-conjugation in C-C bonds close to the typical aromatic C-C bond of 1.39 Å.

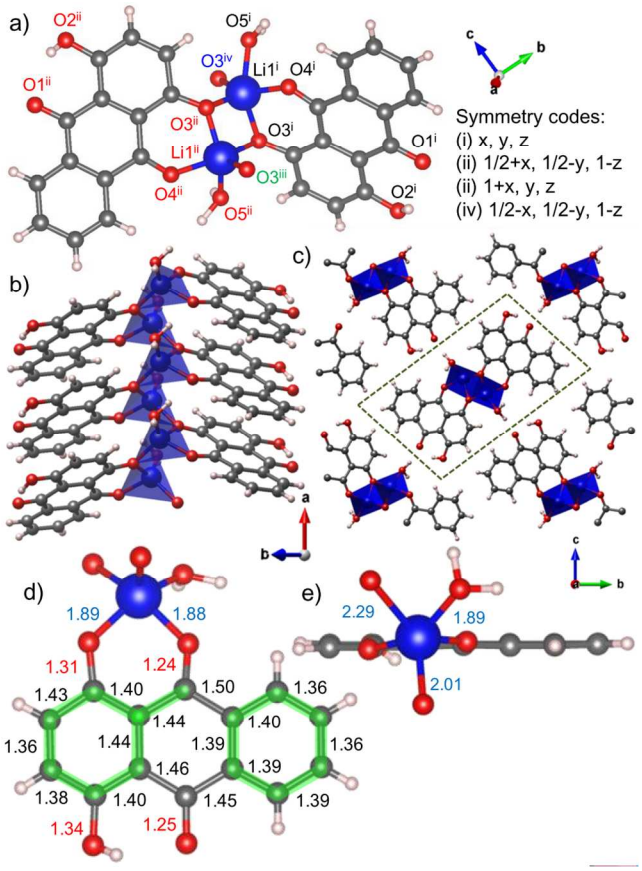

Fig. 6 Crystal structure of **5** [Li(14dhaqH)(H_2O)]. H (white), Li (blue), C (grey), O (red). (a-c) 1D inorganic chains composed of LiO_5 are formed along the *a* axis with the anthraquinone parts stacked along the same direction. These chains are separated from each other as shown by the dashed box in the panel (c). (d, e) Coordination environments and bond lengths determined at room temperature. The blue numbers are Li-O bond lengths in Å, the red ones are C-O bond lengths, and the black ones are C-C bond lengths. The green highlights illustrate strong π-conjugation in C-C bonds close to the typical aromatic C-C bond of 1.39 Å.

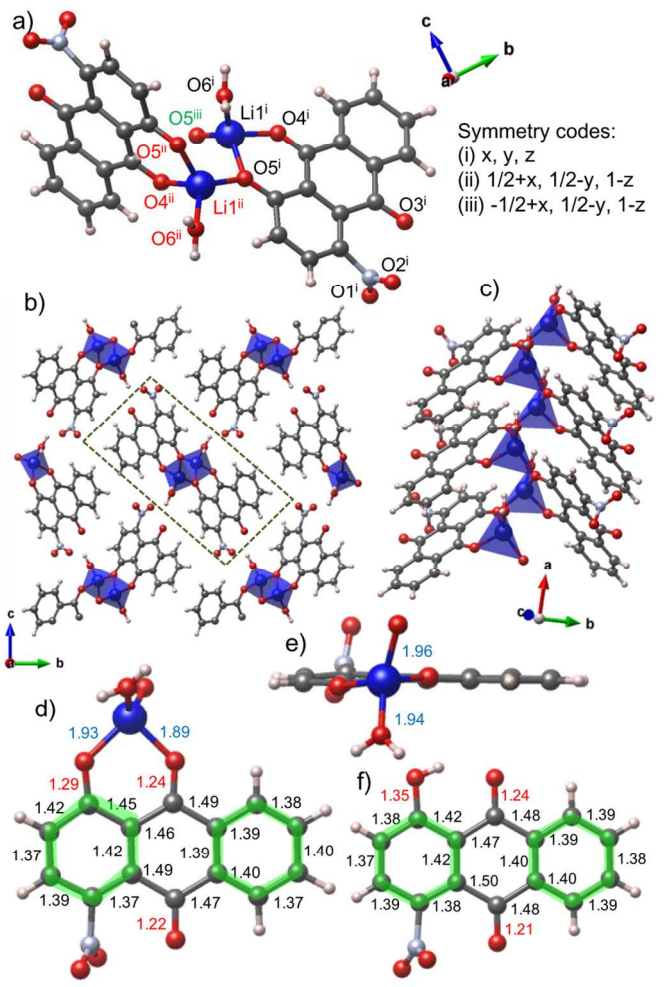

Fig. 7 Crystal structure of **6** [Li(14hnaqH)(H_2O)], isostructural with compound **5**. H (white), Li (blue), C (grey), O (red). (a-c) LiO_4 forms inorganic chains along the *a* axis with the anthraquinone parts stacked along the same direction. These chains are separated from each other as shown by the dashed box in the panel (b). (d, e) Coordination environments and bond lengths determined at room temperature, compared with the data for a protonated linker molecule (f) determined by SXRD. The blue numbers are Li-O bond lengths in Å, the red ones are C-O bond lengths, and the black ones are C-C bond lengths. The green highlights illustrate strong π-conjugation in C-C bonds close to the typical aromatic C-C bond of 1.39 Å.

3.4 Optical absorption and conductivity measurements

UV-vis spectra were recorded for compounds **1** and **3-6** and the parent aq derivatives. In the case of dcaq-based **1**, the mid-point of the optical band edge is red-shifted by 0.3 eV to 3.2 eV upon LCP formation (Fig. S11a). In the case of hydroxyl-aq-based **3-6**, the effect of LCP formation was more pronounced, with red-shifts of 0.35–0.7 eV leading to optical band edges of 1.6–2.1 eV (Fig. S11b-d). This effect may be due to the difference in delocalization of the negative charge or the higher degree of π-stacking in **3-6**, which has been shown to increase red-shifts in the fluorescence spectra of polymorphs of semiconducting 8-tris-hydroxyquinoline aluminium (Alq_3).[40]

1-D π-π stacking is a general feature of the aq-based LCPs, helping to direct and stabilize the crystal packing. This stacking

and the relatively low optical band gaps of **1** and **3**-**6** (for comparison, the optical band gap of Alq_3 is 2.7 eV) suggested the possibility of electronic conductivity or semiconductivity. Conductivity measurements on single crystals[41] revealed insulating behaviour in all cases. In semiconducting polymers and molecular materials, the size of the electronic band gap is equal to the optical band gap plus an additional contribution from the exciton binding energy, required to delocalize the somewhat localized charge carriers. The magnitude of the exciton binding energy is usually about 0.3-0.4 eV, but in systems such as Alq_3 it may be as high as 1.4 eV.[42, 43] The fact that the anthraquinone-based LCPs are insulating suggests that, despite the extended framework connectivity and π-stacking, their exciton binding energies are even higher, i.e. charge delocalization is even more limited than in Alq_3.

A simple analysis of bond orders (i.e., the degree of single- or double-bond character based on electron counting) in the aq derivatives, which agrees well with the bond lengths determined by single crystal X-ray diffraction, confirmed that π-conjugation is indeed more localized in aq-based LCPs compared to Alq_3 (See ESI Section 11). The HOMO and LUMOs of the aq-derivatives are expected to be located predominantly around the electronegative oxygen atoms, with little delocalization across the whole aq ring system. This is in contrast to 8-tris-hydroxyquinoline and anthracene itself, in which resonance in the π-system describes well the delocalization of HOMO and LUMO across all the aromatic rings.

3.5 Origin of the correlation and importance of the exceptions

The effective coordination number (ECoN) and tetrahedral distortion values (δ_{tet}) (Table S2-S4) suggest that LiO_4 tetrahedra are formed perfectly even for such rigid organic linkers, resulting in a lack of ionic conductivity. These LCPs are mostly synthesized from solution, thus LiO_4 tetrahedra are considered to form even before crystallization and this in turn means that only such units can be crystallized. This may be the reason why there are lots of structures having the LiO_4 coordination dominated by negative charge of one coordination group. These coordination spheres have short Li-O bonds, and thus the positive charge of Li^+ ions is considered to be well compensated.

By comparison, a crystalline lithium conductor $Li(PF_6)$:(poly(ethylene oxide))$_6$ contains 5-coordinate Li with bond lengths all over 2.1 Å, giving an ECoN of 5.0.[44] In order to obtain interesting properties such as Li^+ conduction, it is therefore better to form weakly-coordinated Li^+ sites as discussed in oxides,[8] that is, to form Li coordination spheres not following the correlation described in Fig. 1, together with adequate pathways for ion migration through the structure, such as Li vacancies.[45]

By using other crystallization routes, we can obtain different coordination environments. For example, a dense coordination polymer, $(dma)_2[Li_2(Zr(ox)_4)]$ (dma = $(CH_3)_2NH_2^+$ and ox = $C_2O_2^{2-}$), which has isolated LiO_4 tetrahedra, can be transformed into $(dma)_2[Li_2(H_2O)_{0.5}(Zr(ox)_4)]$, which has LiO_5 inorganic chains, by a topotactic hydration reaction.[21] The former was synthesized by a solvothermal reaction and the ECoN values of the Li-O coordination environments are 3.99 and 4.00, while the values in the latter are extremely high, 4.78, 4.54, 4.50 and 4.87. Such high ECoN values are also found in hydrated lithium tartrates, which commonly exhibit Li-O bond lengths above 2.0 Å (Table S6), suggesting that hydration may be a more general strategy to destabilize Li coordination spheres. However, it should be noted that incorporation of water and other small guest molecules limits the high temperature stability and performance of coordination polymers. Unusual coordination environments were often found in classical solid-state materials synthesized via a topochemical route.[46, 47] Since such topochemically synthesized materials are known to exhibit unique properties,[48, 49] post synthetic treatments of this type are considered to be an important strategy for achieving unique properties in LCPs and MOFs.[41]

4. Conclusions

We found that there is a weak linear correlation in LCPs between the longest C-O bonds in the coordinating organic anions and the shortest Li-O bonds, unless there is hydrogen bonding to the oxygen atoms, the lithium ECoN values are above 4.0, or the Li-O bonds are not the shortest in the Li-O coordination spheres of interest. The correlation indicates that the LiO_4 coordination is dominated by the negative charge of one coordinating group, which probably originates from the crystallization routes.

Regarding properties of LCPs, despite exhibiting optical band edges below 2 eV and 1-D π-stacking connectivity in aq-based LCPs, conductivity measurements on single crystals of **1**-**6** confirmed that they are all electronic insulators. We rationalize this finding on the basis of π-orbital delocalization, which is more restricted in the aq-based LCPs compared to known semiconducting hybrid materials. These aq-based LCPs are also not lithium conductive. This is reasonable considering the short Li-O bonds in the coordination spheres where the correlation between bond lengths was found. In order to obtain lithium conductive LCPs, our findings suggest that crystallization where one negative charge does not dominate the coordination environments and post synthetic treatments are promising.

Acknowledgements

This work was supported by an Advanced Investigator Award from the European Research Council, ERC, (to AKC) and the World Premier International Research Center Initiative on "Materials Nanoarchitectonics (WPI-MANA)" from MEXT, Japan. SH thanks the Alexander von Humboldt Foundation for funding. We thank the EPSRC UK National Crystallography Service at the University of Southampton for the collection of the crystallographic data (compound **5** and **6**).

Notes and references

[a] International Center for Materials Nanoarchitectonics, National Institute for Materials Science, Ibaraki 305-0044, Japan.

[b] Department of Materials Science and Metallurgy, University of Cambridge, Cambridge CB3 0FS, United Kingdom.
[c] Lehrstuhl für Anorganische Chemie II, Ruhr-Universität Bochum, 44780 Bochum, Germany.

† Electronic Supplementary Information (ESI) available: [Details of synthesis. Thermogravimetric analyses. Powder XRD]. See DOI: 10.1039/b000000x/

‡ CCDC 1419034-1419050 contain the supplementary crystallographic data for this paper. These data can be obtained free of charge from The Cambridge Crystallographic Data Centre via www.ccdc.cam.ac.uk/data_request/cif.

1. B. Scrosati and J. Garche, *J. Power Sources*, 2010, **195**, 2419-2430.
2. M. Armand and J. M. Tarascon, *Nature*, 2008, **451**, 652-657.
3. H. Chen, M. Armand, G. Demailly, F. Dolhem, P. Poizot and J. M. Tarascon, *ChemSusChem*, 2008, **1**, 348-355.
4. H. Y. Chen, M. Armand, M. Courty, M. Jiang, C. P. Grey, F. Dolhem, J. M. Tarascon and P. Poizot, *J. Am. Chem. Soc.*, 2009, **131**, 8984-8988.
5. A. L. Barres, J. Q. Geng, G. Bonnard, S. Renault, S. Gottis, O. Mentre, C. Frayret, F. Dolhem and P. Poizot, *Chem. A. Euro. J.*, 2012, **18**, 8800-8812.
6. M. Armand, S. Grugeon, H. Vezin, S. Laruelle, P. Ribiere, P. Poizot and J. M. Tarascon, *Nat. Mater.*, 2009, **8**, 120-125.
7. R. E. Dinnebier, H. Nuss and M. Jansen, *Z. Kristallogr*, 2005, **220**, 954-961.
8. P. G. Bruce, ed., *Solid State Electrochemistry*, Cambridge University Press, Cambridge, 1995.
9. A. Enders-Beumer and S. Harkema, *Acta. Crystallogr.*, 1973, **B29**, 682.
10. J. L. Galigne, M. Louvet and J. Falgueirettes, *Acta. Crystallogr.*, 1970, **B26**, 368.
11. F. J. M. Casado, M. R. Riesco, M. I. Redondo, D. Choquesillo-Lazarte, S. Lopez-Andres and J. A. R. Cheda, *Cryst. Growth Des.*, 2011, **11**, 1021-1032.
12. B. Beagley and R. W. H. Small, *Acta Crystallogr.* , 1964, **17**, 783-788.
13. H. H. M. Yeung and A. K. Cheetham, *Dalton Trans.*, 2014, **43**, 95-102.
14. H. H. M. Yeung, M. Kosa, M. Parrinello and A. K. Cheetham, *Cryst. Growth Des.*, 2013, **13**, 3705-3715.
15. H. H. M. Yeung, M. Kosa, M. Parrinello, P. M. Forster and A. K. Cheetham, *Cryst. Growth Des.*, 2011, **11**, 221-230.
16. J. A. Kaduk, *Acta Cryst.* , 2000, **B56**, 474-485.
17. B. F. Abrahams, M. J. Grannas, T. A. Hudson and R. Robson, *Angew. Chem. Int. Ed.*, 2010, **49**, 1087-1089.
18. X. Zhao, T. Wu, S. T. Zheng, L. Wang, X. H. Bu and P. Y. Feng, *Chem. Commun.*, 2011, **47**, 5536-5538.
19. S. T. Zheng, Y. F. Li, T. Wu, R. A. Nieto, P. Y. Feng and X. H. Bu, *Chem. A. Euro. J.*, 2010, **16**, 13035-13040.
20. D. Banerjee and J. B. Parise, *Cryst. Growth Des.*, 2011, **11**, 4704-4720.
21. S. Tominaka, F. X. Coudert, T. D. Dao, T. Nagao and A. K. Cheetham, *J. Am. Chem. Soc.*, 2015, **137**, 6428-6431.
22. P. A. Cox, *Transition Metal Oxides: An introduction to their electronic structure and properties*, Clarendon Press, Oxford, 1992.
23. G. M. Sheldrick, *Acta Cryst. Sec. A*, 2008, **64**, 112-122.
24. O. V. Dolomanov, L. J. Bourhis, R. J. Gildea, J. A. K. Howard and H. Puschmann, *J. Appl. Cryst.*, 2009, **42**, 339-341.
25. A. G. Csaszar, G. Czako, T. Furtenbacher, J. Tennyson, V. Szalay, S. V. Shirin, N. F. Zobov and O. L. Polyansky, *J. Chem. Phys.*, 2005, **122**, 21430501-21430510.
26. K. Momma and F. Izumi, *J. Appl. Cryst.*, 2011, **44**, 1272-1276.
27. C. F. Macrae, I. J. Bruno, J. A. Chisholm, P. R. Edgington, P. McCabe, E. Pidcock, L. Rodriguez-Monge, R. Taylor, J. van de Streek and P. A. Wood, *J. Appl. Cryst.*, 2008, **41**, 466-470.
28. H. H. M. Yeung, W. Li, P. J. Saines, T. K. J. Koster, C. P. Grey and A. K. Cheetham, *Angew. Chem. Int. Ed.*, 2013, **52**, 5544-5547.
29. P. J. Saines, J. C. Tan, H. H. M. Yeung, P. T. Barton and A. K. Cheetham, *Dalton Trans.*, 2012, **41**, 8585-8593.
30. M. Sorianogarcia and S. N. Rao, *Acta Cryst. Sec. C*, 1983, **39**, 850-852.
31. Y. Idemoto, J. W. R. Jr., N. Koura, S. Kohara and C.-K. Loong, *J. Phys. Chem. Solids*, 1998, **59**, 363-376
32. J. McMurry, *Organic Chemistry (5th ed)*, Brooks/Cole, USA, 2000.
33. C. Giacovazzo, H. L. Monaco, G. Artioli, D. Viterbo, M. Milanesio, G. Ferraris, G. Gilli, P. Gilli, G. Zanotti and M. Catti, *Fundamentals of Crystallography*, Oxford University Press, Oxford, 2011.
34. A. K. Cheetham, C. N. R. Rao and R. K. Feller, *Chem. Commun.*, 2006, 4780-4795.
35. The dimensionality of the hybrid systems is described in terms of both the inorganic connectivity (I^n) and organic connectivity (O^m).
36. A. K. Cheetham, C. N. R. Rao and R. K. Feller, *Chem. Commun.*, 2006, 4780-4795.
37. J. D. Furman, R. P. Burwood, M. Tang, A. A. Mikhailovsky and A. K. Cheetham, *J. Mater. Chem.*, 2011, **21**, 6595-6601.
38. S. Tominaka and A. K. Cheetham, *RSC Adv.*, 2014, **4**, 54382-54387.
39. S. Tominaka, S. Henke and A. K. Cheetham, *CrystEngComm*, 2013, **15**, 9400-9407.
40. M. Brinkmann, G. Gadret, M. Muccini, C. Taliani, N. Masciocchi and A. Sironi, *J. Am. Chem. Soc.*, 2000, **122**, 5147-5157.
41. S. Tominaka, H. Hamoudi, T. Suga, T. D. Bennett, A. B. Cairns and A. K. Cheetham, *Chem. Sci.*, 2015, **6**, 1465-1473.
42. M. Knupfer, H. Peisert and T. Schwieger, *Phys. Rev. B*, 2002, **65**.
43. I. G. Hill, A. Kahn, Z. G. Soos and R. A. Pascal, *Chemical Physics Letters*, 2000, **327**, 181-188.
44. Z. Gadjourova, D. M. Marero, K. H. Andersen, Y. G. Andreev and P. G. Bruce, *Chemistry of Materials*, 2001, **13**, 1282-1285.
45. Y. Y. Zhang, Y. Y. Sun, S. X. Du, H. J. Gao and S. B. Zhang, *Appl. Phys. Lett.*, 2012, **100**.
46. M. A. Hayward, M. A. Green, M. J. Rosseinsky and J. Sloan, *J. Am. Chem. Soc.*, 1999, **121**, 8843-8854.
47. Y. Tsujimoto, C. Tassel, N. Hayashi, T. Watanabe, H. Kageyama, K. Yoshimura, M. Takano, M. Ceretti, C. Ritter and W. Paulus, *Nature*, 2007, **450**, 1062-1065.
48. S. Tominaka, H. Yoshikawa, Y. Matsushita and A. K. Cheetham, *Mater. Horiz.*, 2014, **1**, 106-110.
49. S. Tominaka, *Inorg. Chem.*, 2012, **51**, 10136-10140.

Coordination Environments and π-Conjugation in Dense Lithium Coordination Polymers

Satoshi Tominaka, Hamish H.-M. Yeung, Sebastian Henke and Anthony K. Cheetham

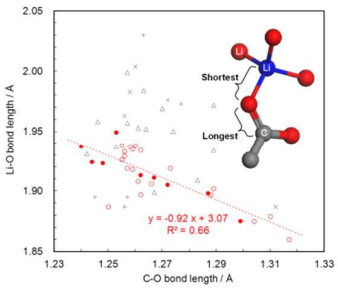

A weak relationship between the longest C-O bond in the anionic organic ligand and the shortest Li-O bond was found.